Available online at www.sciencedirect.com
SCIENCE DIRECT®
Polymer 45 (2004) 3595–3608
polymer
www.elsevier.com/locate/polymer

First-principles calculation of particle formation in emulsion polymerization: pseudo-bulk systems

Emma M. Coen[a], Sarah Peach[b], Bradley R. Morrison[b], Robert G. Gilbert[a,*]

[a]*Key Centre for Polymer Colloids, Chemistry School F11, University of Sydney, Sydney, NSW 2006, Australia*
[b]*BASF ZKD, BASF ZK-Kunststofflaboratorium B 1, Polymer Research Division, BASF Ludwigshafen D-67056, Germany*

Received 26 December 2003; received in revised form 23 March 2004; accepted 26 March 2004

Abstract

Kinetic behavior in emulsion polymerization can be conveniently assigned as either 'zero-one' or 'pseudo-bulk'. Sufficiently small particles in emulsion polymerizations obey zero-one kinetics, where entry of a radical into a particle which contains a growing radical leads to instantaneous termination. Pseudo-bulk kinetics applies to particles in which more than one free radical can co-exist for a significant period; while this is commonly applicable to large particles for any monomer, it also applies to very small particles for monomers which propagate very rapidly, such as acrylates. A methodology is developed to enable particle sizes and rates to be calculated for systems in which pseudo-bulk kinetics are important during particle formation. This takes account of all significant reactions involving radical species in the water and particle phases, including the chain-length dependence of the termination rate coefficient. A 'cross-over radius' r_{co} is used to describe the particle size where termination of radicals within the particles is no longer instantaneous. The model is applied to the emulsion polymerization of butyl acrylate. All parameters are available from the literature, except for r_{co} and k_p^1, the rate coefficient for propagation of a monomeric radical formed from transfer. These were determined from experiments on seeded emulsion polymerizations of this monomer, involving the steady-state rate with chemical initiator and non-steady-state rate in a system initiated by γ radiolysis, after removal from the radiation source ('relaxation' mode). Particle sizes and rates in unseeded butyl acrylate emulsion polymerizations at 50 °C, over a range of concentrations of persulfate as initiator and sodium dodecyl sulfate as surfactant, are predicted by the model with acceptable accuracy.

Keywords: Polymer chemistry; Polymer synthesis; Polymer materials

1. Introduction

Models for particle formation in emulsion polymerization, which are capable of predicting quantities such as particle size and rates using a minimum of fitting parameters, are useful both for designing 'recipes' to give desired outcomes, and to help test mechanistic hypotheses. There are many models for particle formation in the literature, e.g. [1–24], but (without going into exhaustive discussion of these cited approaches), none have the mechanistic completeness of that developed here. This is the first that includes all of the following mechanisms, some of which have been established only relatively recently. Most are summarized in Fig. 1, which incorporates various aspects of earlier work [2,3,5,7–11,25–28]).

- Radicals arising directly from initiator propagate with the small amount of monomer in the water phase, until they reach a degree of polymerization z, when they become surface active; aqueous-phase propagation can occur with all degrees of polymerization less than z.
- There are three fates of z-mers: entry into a pre-existing particle, entry into a (monomer-swollen) micelle, or further propagation and termination until attaining a critical degree of polymerization j_{crit}.
- Particle formation occurs only through entry of a z-mer into a micelle, or by collapse (precipitation) of a j_{crit}-mer (micellar and homogeneous nucleation, respectively).
- Termination between radicals, for which the rate coefficient depends on the lengths of each terminating chain.
- Transfer of radical activity from a propagating chain to monomer; the resulting monomeric radical may either propagate or desorb out of and away from the particle: the process of exit.

* Corresponding author. Tel.: +61-2-9351-3366; fax: +61-2-9351-8651.
E-mail address: gilbert@chem.usyd.edu.au (R.G. Gilbert).

0032-3861/$ - see front matter © 2004 Elsevier Ltd. All rights reserved.
doi:10.1016/j.polymer.2004.03.084

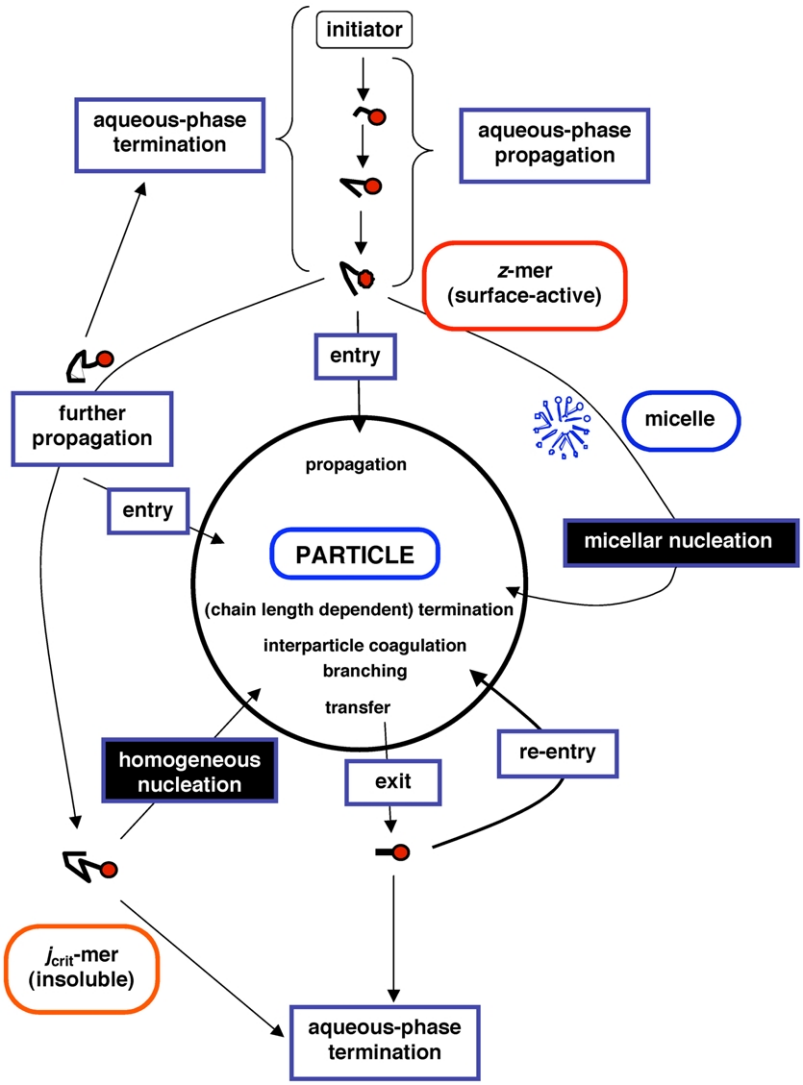

Fig. 1. Some kinetic events in emulsion polymerization, including the competing paths for particle formation and for particle growth.

- Re-entry of desorbed radicals into (another) particle.
- Small particles (especially those which have just formed) are relatively unstable colloidally, and may coagulate.
- An important, although non-mechanistic, aspect of modeling is that values of many rate coefficients for many monomers are known with precision (e.g. that for propagation using pulsed-laser polymerization), and therefore cannot be either treated as adjustable parameters (or, equivalently, be assigned a convenient value from the wide range reported in tabulations which have not been subjected to critical evaluation [29]).

1.1. Micellar nucleation

In a system which has added surfactant, the dominant fate of new z-meric radicals while/if micelles are present is to enter a micelle, because micelles have a high number density. Hence, new particle formation continues while micelles are present. Micelles disappear when sufficient surfactant has become adsorbed onto pre-existing particles, which requires a sufficiently large number of particles with sufficient size. This takes some time, and thus particle formation is a relatively extended process. Hence, the number of particles is large (i.e. the final particle size is comparatively small): a typical feature of micellar nucleation.

1.2. Homogenous nucleation

In systems where there is insufficient free surfactant to form micelles, z-meric radicals may enter a pre-existing particle, or terminate in the water phase, or propagate further to j_{crit}-mers to form new particles. Once enough particles are present, then a likely fate of new z-mers is to enter these, rather than propagate on to j_{crit}-mers. Thus, in a system without (or with very little) surfactant, particle formation finishes quickly, and hence the number of

particles is small (i.e. the final particle size is large): a typical feature of homogeneous nucleation.

All of these effects have been incorporated into a model which has been published previously [19], except that of chain-length-dependent termination. As will be seen, this last effect is important for monomers such as acrylates. Means of incorporating this effect, and one set of experiments which can be used to fit some parameters, and an independent set of experiments which can be used to test the model, form the subject of the present paper.

A significant aspect of the work given here is in the classification of approximations used to handle the kinetics. An important phenomenon in emulsion polymerization kinetics is *compartmentalization*: the main locus of polymerization is within the particles, and these particles spatially segregate radicals from each other. This can have major effects on both rates and on molecular weight distributions (including in controlled-radical polymerization in dispersed media [30]). Consider for example, a hypothetical system containing only particles with a single polymeric radical inside each particle. Because of the isolation of radicals in the particles, these radicals cannot terminate directly with each other, whereas they would undergo termination in a bulk or solution system with the same overall radical concentration. For this reason, in quantifying emulsion polymerization kinetics, it is necessary to treat particles containing zero, one, two, etc. growing chains as separate species [4], with populations N_0, N_1, N_2, etc. The complexity does not stop there, because (a) there is the possibility of exit of a monomeric free radical formed by transfer, and (b) the rate coefficient for termination depends on the degrees of polymerization of each terminating radical (chain-length-dependent termination). For this reason, it is necessary in general to distinguish particles not only by the number of growing radicals they contain, but by the distribution of the degrees of polymerization of each of these radicals, N', N'', N''' [31]. This leads to an infinitely hierarchical description of the variables, e.g. $N_2(N',N'')$, $N_3(N',N'',N''')$, etc. The only exact way of solving this infinite hierarchy of equations is to abandon the evolution equation approach and turn instead to Monte-Carlo modeling (e.g. [30,32]). While Monte-Carlo modeling enables this complexity to be handled, the enormous computational time required (typically days for a single calculation, even on a distributed network of linked computers [30]) precludes its use in routine interpretation and prediction of experiment.

The best means developed so far to overcome this impasse is to define two limiting, but widely applicable, categories to describe emulsion polymerization kinetics: 'zero-one' and 'pseudo-bulk', as approximations to the true kinetics. A zero-one system is one in which entry of a radical into a particle which already contains a growing radical results in 'instantaneous' termination. Such systems can never contain more than one radical per particle, and intra-particle termination is not a rate-determining step; hence chain-length-dependent events can be handled in a simple fashion. The other extreme is a pseudo-bulk system, where for a number of reasons [8,33,34] the kinetics are formally identical to those in a bulk or solution free-radical polymerization, and thus it is only necessary to take account of the distribution of degrees of polymerization of growing chains. In each case, the resulting evolution equations are relatively simple to write down and solve (e.g. [31,34,35]), and can thus be used for the routine prediction and interpretation of appropriate experimental data.

Typically, small particles exhibit zero-one kinetics, and large particles exhibit pseudo-bulk kinetics. Pseudo-bulk kinetics are also exhibited by small particles, if exited radicals rapidly re-enter and re-exit other particles, in which case the compartmentalization has no formal kinetic effect [8]; this latter case is applicable for monomers such as methyl methacrylate and butyl acrylate (BA), except very small particles. The size range over which pseudo-bulk kinetics are applicable is quantified in a later section, but at this point it is noted that if the propagation rate coefficient (k_p) is high, then pseudo-bulk kinetics are likely to be inapplicable except for very small particles. It is apparent that newly nucleated particles, being extremely small, are likely to obey zero-one kinetics, but if they have a high k_p (as does MMA to some extent, while BA has an extremely high k_p [36,37]), then they are very likely to cross over to pseudo-bulk kinetics while still relatively small, and hence, while nucleation is likely to be continuing.

The present paper extends the work cited above [19] which incorporated all of the effects listed except chain-length-dependent termination into nucleation modeling: the present paper shows how to allow for pseudo-bulk kinetics in the particle formation step.

In Section 2, we review the formulation of nucleation kinetics for the zero-one case [19], and then give the corresponding formulation for pseudo-bulk kinetics. We then develop a means to handle the crossover between zero-one and pseudo-bulk kinetics. The modeling is related to experiment using new data for the ab initio (unseeded) and seeded emulsion polymerization of butyl acrylate (a small polystyrene seed being used as host for BA for this purpose).

2. Model for particle formation and growth

The events in particle formation and growth are as follows (Fig. 1). Initiator decomposes in the aqueous phase, forming radicals, which then react with monomer to form oligomeric radicals in the aqueous phase. These oligomeric radicals can propagate or terminate. If the oligomeric radicals are larger than the critical degree of polymerization for entry (z) [38], they may enter a pre-existing particle (entry frequency per particle ρ) or enter micelles if micelles are present in the system (note that 'frequency' is the correct IUPAC terminology [39] for the rate parameters for entry and exit, formerly called 'entry and exit rate coefficients'). Oligomeric radicals whose degree of polymerization is

above the critical size for homogeneous nucleation (j_{crit}) collapse to form a particle. Radicals within particles can terminate, propagate or transfer radical activity to monomer (rate coefficient k_{tr}). The monomeric radical generated by chain transfer may propagate within the particle, or exit the particle by diffusion into the water phase, whereupon it may re-enter another particle, or enter a micelle, forming a new particle. Termination of radicals in the particles may be 'instantaneous' [40] (zero-one kinetics) or may be rate-determining (pseudo-bulk kinetics). Another competing path for particle formation is the entry of oligomeric radicals into monomer droplets, but this is usually negligible (the exceptions being monomers such as chlorobutadiene [41] and in ab initio controlled-radical polymerization [42,43]). Many parameters are size-dependent, such as the concentration of monomer in particles (C_p) and the entry and exit frequencies. Because of this, a complete model requires computation of the evolution of the full particle size distribution.

Compartmentalization of radicals is included by distinguishing particles according to the number of radicals they contain. Since monomeric radicals formed by transfer are able to undergo exit (desorption) into the aqueous phase, unlike the larger polymeric radicals [44–46], it is necessary to take into account whether the radicals in the latex particles are polymeric or monomeric.

Transfer to polymer is neglected in this model. This effect may, however, be important in the case of butyl acrylate polymerization, since it leads to both short-chain branching through back-biting and long-chain branching by transfer to a distant part of another (or the same) chain. This probably has major effects on the overall kinetics of BA polymerization, because the radical center formed by transfer may have a low rate coefficient for addition to a monomer unit, which can affect the apparent value of k_p [47–50]. In the present paper, an effective k_p is assumed to take such effects into account.

As stated, the treatment requires the time evolution of the full particle size distribution to be computed. It is assumed here that it is sufficiently accurate to assume that there exists a 'cross-over radius' r_{co} such that particle growth is governed by zero-one kinetics below r_{co}. Above r_{co}, particle growth is governed by pseudo-bulk kinetics, when termination within the particles is rate-determining. Coagulation is not included above r_{co} because of considerable added complexity in the evolution equations; this is acceptable because particles bigger than r_{co} are probably large enough to be colloidally stable.

In describing particle size distributions, one must distinguish swollen and unswollen size. Particles are swollen with monomer, and the unswollen volume of a particle (i.e. its volume in the absence of monomer) is equivalent to the mass of polymer in the particle. The swollen volume V_s and unswollen volume V are trivially related by mass conservation (assuming ideal mixing of monomer and polymer):

$$\frac{V_s}{V} = \frac{d_M}{d_M - C_p M_0} \tag{1}$$

where d_M is the density of monomer and M_0 is the molecular weight of the monomer. Whether one uses swollen or unswollen volume, or equivalently swollen or unswollen radius, r_s and r, is a matter of convenience: for example, as will be seen the particle-size distribution equations are most compactly set out in terms of unswollen volume (because the change in unswollen particle volume with polymer growth is linear), whereas coagulation rate coefficients are most conveniently calculated in terms of swollen volume.

A physically realistic model for particle formation requires one to take into account the occurrence of coagulation involving very small particles. The basic reason for this is that tiny particles, as are formed as a result of micellar and homogenous nucleation, have highly curved double layers and are thus likely to be colloidally unstable to both hetero- and homo-coagulation (e.g. [51,52]). Particles grow through the propagation of radicals within the particle or, if colloidally unstable, by coagulation [3,53]. $B(V, V')$ denotes the rate coefficient for coagulation between two particles of volume V and V'.

The total number of particles per unit volume of the continuous phase, N_p, is given by:

$$\frac{N_p}{N_A} = \int_0^\infty n(V)\mathrm{d}V \tag{2}$$

where N_A is Avogadro's constant and $n(V)$ is the molar concentration of particles with unswollen volume V. The particle number and particle size are related by:

$$N_p = \frac{\text{mass polymer}}{\frac{4}{3}\pi r^3 d_P} \tag{3}$$

where d_P is the density of polymer. The particle size distribution in terms of volume, $n(V)$, and radius, $n_r(r)$, are related by [54]:

$$n(V) = \frac{n_r(r)}{4\pi r^2} \tag{4}$$

The Morton–Flory–Huggins treatment [55] suggests that C_p should be a function of particle size, with significant variation for very small particles. Here, the following functional form is assumed [19]:

$$C_p(r) = C_p^\infty \tanh\left(\frac{r}{r_F}\right) \tag{5}$$

where r_F expresses the radius at which $C_p(r)$ rapidly approaches the limiting value C_p^∞. This functional form is computationally convenient and provides a good fit to the form predicted by the Morton equation [55]. It is noted that the Morton equation cannot be used predictively, so Eq. (5), although empirical, provides an equally valid quantification of this dependence.

2.1. Zero-one regime

In a zero-one system, the evolution of particle size distributions for particles containing no radicals, one monomeric radical, and one polymeric radical are considered separately The total population of particles is:

$$n(V) = n_0(V) + n_1^{\mathrm{M}}(V) + n_1^{\mathrm{P}}(V) \tag{6}$$

where $n_1^{\mathrm{M}}(V)$ is the molar concentration of particles of a volume V that contain one monomeric radical; $n_1^{\mathrm{P}}(V)$ is the molar concentration of particles of a volume V that contain one polymeric radical, and $n_0(V)$ is the molar concentration of particles of unswollen volume V that contain zero radicals.

The equations that describe the time evolution of the particle size distribution for a zero-one system take into account the following events. A particle containing no radicals can gain a polymeric radical through the propagation of a monomeric radical, entry of an oligomeric radical, or coagulation with a particle containing a polymeric radical. The evolution equation is as follows [7,19,34].

$$\begin{aligned}\frac{\partial n_0(V,t)}{\partial t} &= \rho(V)[n_1^{\mathrm{M}} + n_1^{\mathrm{P}} - n_0] + k_{\mathrm{dM}} n_1^{\mathrm{M}} - n_0 \int_0^{\infty} \\ &\quad \times B(V, V')[n_0(V') + n_1^{\mathrm{P}}(V')]\mathrm{d}V' k_{\mathrm{eE}}[\mathrm{E}] \\ &\quad + \int_0^{\infty} B(V, V - V')[n_0(V')n_0(V - V') \\ &\quad + n_1^{\mathrm{P}}(V')n_1^{\mathrm{P}}(V - V')]\mathrm{d}V' \end{aligned} \tag{7}$$

where ρ is the entry frequency:

$$\begin{aligned}\rho(V) &= \rho_{\mathrm{spont}} + \rho_{\mathrm{initiator}}(V) + k_{\mathrm{eE}}(V)[\mathrm{E}]; \\ \rho_{\mathrm{initiator}} &= \sum_{i=z}^{j_{\mathrm{crit}}-1} k_{\mathrm{e}}^{i}(V)[\mathrm{IM}_i]\end{aligned} \tag{8}$$

Here, ρ_{spont} is the contribution to entry from radicals produced spontaneously, e.g. from decomposition of peroxide species on the seed [41]; it is found to have a very small value in the present butyl acrylate system (see Section 3.1.2), and is needed in the present modeling only for γ-radiolysis relaxation experiments, from which its value can be determined directly. The quantity k_{eE} is the rate coefficient for entry of an aqueous-phase radical E which has resulted from exit from a particle, $[\mathrm{IM}_i]$ is the concentration of i-meric radicals in the aqueous phase, and k_{dM} is the rate coefficient for the desorption of a monomeric radical into the water phase:

$$k_{\mathrm{dM}} = \frac{3D_{\mathrm{w}}}{r_{\mathrm{s}}^2}\frac{C_{\mathrm{w}}}{C_{\mathrm{P}}} \tag{9}$$

where D_{w} is the diffusion coefficient of a monomeric radical in the water phase, and C_{w} is the concentration of monomer in the water phase. Particles can gain radicals through entry, or by coagulation with a particle containing a radical. Particles containing no radicals can be generated from particles containing a radical by the entry of a radical, leading to an instantaneous termination event, or by exit of a monomeric radical. Particles containing no radicals can only increase in size by coagulation. If a particle containing no radicals coagulates with another particle that contains no radicals, then the resultant particle will contain no radicals. If a particle containing a radical coagulates with another particle that contains a radical, then the resultant particle will contain no radicals. Likewise, if a particle containing no radicals coagulates with another particle that contains a radical, then the resultant particle will contain a radical. It is assumed that particles containing one monomeric radical do not take part in the coagulation process, because of the relatively low number of these particles.

Similarly, the evolution equations for particles containing a polymeric radical are:

$$\begin{aligned}\frac{\partial n_1^{\mathrm{P}}(V,t)}{\partial t} &= \rho(V)(n_0 - n_1^{\mathrm{P}}) - (k_{\mathrm{tr}}C_{\mathrm{P}} + \frac{\partial}{\partial V}K)n_1^{\mathrm{P}} \\ &\quad + k_{\mathrm{p}}^{1}C_{\mathrm{P}}n_1^{\mathrm{M}} + \delta(V - V_0) \\ &\quad \times \left([IM_{j_{\mathrm{crit}}-1}]k_{\mathrm{p,w}}C_{\mathrm{w}} + \sum_{i=z}^{j_{\mathrm{crit}}-1}[\mathrm{IM}_i]k_{\mathrm{e,micelle}}^{i}[\mathrm{micelle}]\right) \\ &\quad - n_1^{\mathrm{P}}\int_0^{\infty} B(V, V')[n_0(V') + n_1^{\mathrm{P}}(V')]\mathrm{d}V' \\ &\quad + \int_0^{\infty} B(V, V - V')[n_0(V')n_1^{\mathrm{P}}(V - V') \\ &\quad + n_1^{\mathrm{P}}(V')n_0(V - V')]\mathrm{d}V' \end{aligned} \tag{10}$$

where $k_{\mathrm{p,w}}$ is the propagation rate coefficient in the aqueous phase, $k_{\mathrm{e,micelle}}^{i}$ is the entry rate coefficient for an i-meric radical into a micelle, [micelle] is the concentration of micelles, and V_0 is the size of the particle when it is formed (assumed for convenience to be the size of a micelle; the value of this quantity makes no significant difference to the computed particle size distribution). The micelle concentration is found by mass conservation, given a value for the micellar aggregation number n_{agg} and the assumption that adsorption of surfactant onto pre-existing particles follows a Langmuir adsorption isotherm [19]. K is the rate coefficient of volume growth for a particle containing a single free radical:

$$K(V) = \frac{k_{\mathrm{p}}M_0C_{\mathrm{p}}(r)}{N_{\mathrm{A}}d_{\mathrm{P}}} \tag{11}$$

The evolution equation for particles containing a monomeric radical is:

$$\frac{\partial n_1^{\mathrm{M}}(V,t)}{\partial t} = -(\rho + k_{\mathrm{p}}^1 C_{\mathrm{p}} + k_{\mathrm{dM}}) n_1^{\mathrm{M}} + k_{\mathrm{eE}}[\mathrm{E}] n_0 + k_{\mathrm{tr}} C_{\mathrm{p}} n_1^{\mathrm{P}} \tag{12}$$

where k_{p}^1 is the propagation rate coefficient for a monomeric radical in the particle phase, and k_{eE} is the rate coefficient for re-entry of an exited radical E into a particle. Particles can gain monomeric radicals by transfer, or the re-entry of an exited radical. Particles can lose a monomeric radical by entry of another radical and the subsequent termination, by the propagation of the radical to form a polymeric radical or by the monomeric radical desorbing.

Eqs. (7)–(12) describe particles formed by homogeneous nucleation and micellar nucleation, and kinetic events within the particles such as propagation, transfer to monomer, entry and exit of oligomeric radicals.

The aqueous–phase species obey the following evolution equations (see Fig. 1):

$$\frac{\mathrm{d}[\mathrm{IM}_1]}{\mathrm{d}t} = 2k_{\mathrm{d}}[\mathrm{I}] - C_{\mathrm{w}} k_{\mathrm{p,w}}^1 [\mathrm{IM}_1] - [\mathrm{IM}_1] \sum_j k_{\mathrm{t,w}} [\mathrm{R}_j] \tag{13}$$

$$\frac{\mathrm{d}[\mathrm{IM}_i]}{\mathrm{d}t} = C_{\mathrm{w}} (k_{\mathrm{p,w}}^{i-1} [\mathrm{IM}_{i-1}] - k_{\mathrm{p,w}}^i [\mathrm{IM}_i]) - [\mathrm{IM}_i] \sum_j k_{\mathrm{t,w}} [\mathrm{R}_j], \quad i = 2, \ldots z-1 \tag{14}$$

where k_{d} is the rate coefficient for dissociation of initiator, $k_{\mathrm{t,w}}$ is the termination rate coefficient of radicals in the water phase (the chain-length dependence of this quantity [28] is ignored here, because of the lack of data on such dependence for small water-phase species), $k_{\mathrm{p,w}}^i$ is the water-phase propagation rate coefficient of a radical of degree of polymerization i, and R_j denotes any aqueous-phase radical of degree of polymerization j (used to include both IM_1 and E as monomeric species). Eq. (13) takes into account the observation that the propagation of an initiator fragment (e.g. $\mathrm{SO_4} - \cdot$) with a monomer is so fast as not to be rate-determining [38,56–61]. The concentration of exited radicals in the water phase is given by:

$$\frac{\mathrm{d}[\mathrm{E}]}{\mathrm{d}t} = \int_0^\infty (k_{\mathrm{dM}}(V) n_1^{\mathrm{M}}(V) - k_{\mathrm{eE}}(V)[\mathrm{E}] n(V)) \mathrm{d}V - [\mathrm{E}] \sum_j k_{\mathrm{t,w}} [\mathrm{IM}_j] \tag{15}$$

The entry rate coefficients are in turn assumed to be diffusion-controlled [62]:

$$k_{\mathrm{e}}^i(V) = 4\pi r_{\mathrm{s}} N_{\mathrm{A}} \frac{D_{\mathrm{w}}}{i^{1/2}}, \quad i \geq z; \qquad k_{\mathrm{e}}^i(V) = 0, \quad i < z \tag{16}$$

$$k_{\mathrm{eE}}(V) = 4\pi r_{\mathrm{s}} N_{\mathrm{A}} D_{\mathrm{w}} \tag{17}$$

where an exponent of 1/2 for the diffusion coefficient of small radicals has been assumed, and it is assumed (as is justified by order-or-magnitude calculations [33]) that the exited radical re-enter without propagating, i.e., its degree of polymerization is 1.

It is important to note that the second-order rate coefficient for radical entry into a particle is proportional to particle radius (as predicted by diffusion-controlled entry of z-mers), not surface area. This inference which is supported by experimental evidence using competitive growth in seeded emulsion polymerizations with bimodal particle size distributions [63]. On the other hand, the (pseudo-first-order) entry frequency in latex with a monodisperse particle size distribution is independent of the radius: i.e. the value of ρ is the same for two separate latexes with different sizes but the same N_{p}, initiator concentration, etc. This inference of the z-mer entry model has been verified experimentally [64]. Both behaviors are predicted by assuming that the entry of a z-mer is diffusion-controlled.

The rate coefficient for radical entry into a micelle (resulting in one of the two modes of particle formation) is given by:

$$k_{\mathrm{e,micelle}}^i = 4\pi r_{\mathrm{micelle}} N_{\mathrm{A}} \frac{D_{\mathrm{w}}}{i^{1/2}}, \quad i \geq z; \qquad k_{\mathrm{e,micelle}}^i = 0, \quad i < z \tag{18}$$

where r_{micelle} is the radius of a micelle.

Of the various rate parameters in this treatment, the only ones whose values are uncertain and to which the calculated rates and particle size distributions are sensitive are k_{p}^1, and the various aqueous-phase propagation rate coefficients $k_{\mathrm{p,w}}^i$. For want of better information, the latter are all assumed to take the value of the long-chain organic-phase k_{p} [36,37]. The value of the propagation rate coefficient of a monomeric radical in the particle phase, k_{p}^1, which is expected to be a few times larger than the long-chain value of k_{p}, will be treated as an adjustable parameter (Section 2.3.3).

2.2. Pseudo-bulk regime

All particles larger than the cross-over radius are considered to grow in a pseudo-bulk fashion. Radicals are no longer isolated within particles, and are not assumed to undergo instantaneous termination should further radicals enter. Propagational growth is controlled by entry of oligomeric radicals and exit of monomeric radicals formed by transfer, and by termination. The rate of growth of particles under the pseudo-bulk regime can be calculated from the rate of growth of the radicals within that particle. In turn, this is determined by the average number of radicals per particle ($\bar{n}$) [34]:

$$\frac{\partial n(V,t)}{\partial t} = -\frac{\partial (K \bar{n} n(V,t))}{\partial V} \tag{19}$$

The value of $\bar{n}$ depends on particle volume. The time evolution of $\bar{n}$ in a particle of volume V in a pseudo-bulk

system is given by [34]:

$$\frac{\partial \bar{n}}{\partial t} = \rho - k\bar{n} - 2\frac{\langle k_t \rangle}{N_A V_s}\bar{n}^2 \tag{20}$$

where all quantities in Eq. (20) may depend on the particle volume. Here, k is the frequency of radical exit from the particle, and $\langle k_t \rangle$ is the average termination rate coefficient, the average being over the chain length distribution of radicals in the particle [28,31,34,65]. The evaluation of $\langle k_t \rangle$ is discussed in Section 2.3.3. The exit frequency is given by [8,33,45]:

$$k = \frac{k_{tr} k_{dM}}{k_p^1} \tag{21}$$

2.3. Implementation

2.3.1. Cross-over radius

The means used here to perform simulations in which pseudo-bulk kinetics is important during particle formation is to assume the existence of a cross-over radius r_{co} such that zero-one kinetics and particle formation occur for all radii less than r_{co}, and pseudo-bulk kinetics are obeyed for $r \geqq r_{co}$. To estimate r_{co} in a given system, it is necessary to estimate the particle size at which there will be a significant fraction of particles containing two growing chains.

The physical reasons for effects of monomer properties and particle size are as follows. First, the radicals are confined within a particle, and therefore zero-one kinetics will become less applicable as the particle size becomes larger. Next, consider the rate coefficient for termination. Termination depends on chain lengths, and is diffusion-controlled. Typical values of the equilibrium concentration of monomer inside a latex particle, in the presence of monomer droplets which provide a reservoir of monomer, are ~ 5 M. Such systems are above the entanglement polymer concentration c^{**} and the monomer/polymer solution is rubbery. In such systems, there is the well-founded belief that the rate of termination is controlled by center-of-mass diffusion of the two terminating chains [28,65–67]. In a system such that the cross-over from zero-one to pseudo-bulk kinetics is taking place, one will have one long growing chain and a short entering chain. Since the longer radical diffuses much more slowly than a short one, the rate of termination will become governed by the diffusion coefficient of the short chain. This will become slower as this oligomeric radical grows by propagation, and thus, all other things being equal, 'instantaneous' termination is less likely for a monomer with a high propagation rate coefficient.

We now make an approximate estimate of the value of the cross-over radius. The region of validity of the 'instantaneous' termination approximation can be estimated by examining the probability of two radicals terminating within a particle, as a function of the degree of polymerization of the shorter chain. Obviously, if there is a very high probability of terminating by the time the short radical has propagated only a few units, then the 'instantaneous' termination approximation will be a good one. This has been formulated by Maeder and Gilbert [68] (note a correction to the original formulation given by Prescott [30]). The probability of a polymeric radical propagating to degree of polymerization j without terminating with an entering freely-moving radical of degree of polymerization z can be calculated as:

$$P_j = \prod_{i=z}^{j-1} \frac{k_p^i C_p}{k_p^i C_p + k_t^{iL}/N_A V_s} \tag{22}$$

where k_p^i is the propagation rate coefficient of an i-meric radical and k_t^{iL} is the termination rate coefficient between a (short) i-meric radical and a long radical. In the present systems, we adopt the diffusion-controlled model for termination [28], which gives:

$$k_t^{iL} = 2p\sigma p_{spin} D_i \tag{23}$$

Here, σ is the radical-center distance at which termination occurs. This is effectively the location of the transition state in this barrierless reaction [69], and can be taken as the van der Waals radius of a monomer unit. The quantity p_{spin} is the probability that both approaching radicals make up a singlet state, and can thus terminate, at distance σ. One has $-\frac{1}{4} \leq p_{spin} \leq 1$, and for rubbery polymer–monomer solutions inside a small particle, $p_{spin} = -\frac{1}{4}$. D_i is the center-of-mass diffusion coefficient of an i-meric radical. This diffusion coefficient depends on the mass-fraction of polymer w_p, and is taken to be given by the scaling expression:

$$D_i = \frac{D_{mon}}{i^{u(w_p)}} \tag{24}$$

The exponent u can be found through experimental studies of oligomers in various polymer matrices over a range of w_p. For methyl methacrylate, butyl methacrylate, hydroxyethyl methacrylate and styrene [70–72] it has been found that u for a wide range of monomer/oligomer/polymer mixtures in the rubbery state can be approximated by the relation:

$$u = 0.664 + 2.02 w_p \tag{25}$$

Fig. 2 shows the probability of an entering radical not terminating, as a function of degree of polymerization, calculated using parameters appropriate for a butyl acrylate system at 50 °C: $k_p^i = 2.4 \times 10^4$ M^{-1} s^{-1}, $i > 1$ [36,73], $k_p^1 = 4.8 \times 10^4$ M^{-1} s^{-1} (using evidence from quantum calculations [74,75] and from measured exit rate coefficients in emulsion polymerizations [76] that the propagation rate coefficient of a monomeric radical is likely to be a few times greater than the long-chain value), $C_p = 5.0$ M (determined by Ruth Gordon in this laboratory by the static swelling method [77]), $D_{mon} = 1.6 \times 10^{-5}$ cm^2 s^{-1} (using the value measured for butyl methacrylate at the corresponding

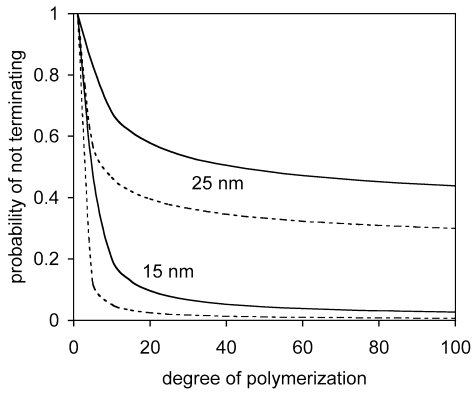

Fig. 2. Calculated probability of a j-mer not terminating before another kinetic event for butyl acrylate, for two swollen particle radii (15 and 25 nm), using the parameter values given in the text. Calculations are for the entering oligomer being trimeric ($z = 3$, applicable to entry of a surface-active radical arising from aqueous-phase propagation of the radical arising from persulfate decomposition [38]; broken line) and monomeric (applicable to re-entry of a monomeric radical resulting from intra-particle transfer followed by exit; full line).

monomer/polymer ratio [70]) and $\sigma = 0.7$ nm. It is apparent from Fig. 2 that a BA particle with swollen radius of 15 nm should obey zero-one kinetics with these input parameters (because the probability of not terminating decreases very rapidly after a small number of monomer units), while one with swollen radius 25 nm is more pseudo-bulk in behavior.

It is noted that the results given in Fig. 2 depend on some parameters whose values are not well established, such as k_p^i for small chains. Moreover, it is impossible to demarcate clearly between pseudo-bulk and zero-one behavior, and indeed any such distinction has some degree of arbitrariness, depending on the property being examined (rates or molecular weight distribution, for example). Although means of bridging this gap by more general treatment of the kinetics, while still taking account of the chain-length dependence of termination, have been developed [30], these are not at present able to be readily incorporated into the full time evolution of the particle size distribution needed to model nucleation kinetics. Because the present approach assumes a clean demarcation in size between pseudo-bulk and zero-one kinetics, the value of the cross-over radius will be treated as a parameter which will be fitted to appropriate data (Section 3.1.1), while keeping in mind that it is expected to be in the range 15–25 nm for butyl acrylate under the experimental conditions used here.

2.3.2. Solution of evolution equations

The method used to solve the coupled integrodifferential equations describing the time evolution of the particle size distribution, together with the rate equations describing the aqueous–phase kinetics, have been described in detail elsewhere [19,34] In brief, the equations in terms of V are converted to those in terms of radius r, and subsequently to finite-difference equations in equal increments of r. The resulting set of coupled ordinary differential equations, of the type d(population in a given radius increment)/dt, are then solved by conventional numerical means. Obtaining adequate resolution in radius and covering a sufficient radius range results in $\sim 10^3$ coupled differential equations for typical conditions. The steady-state approximation is used for all aqueous-phase species and for the populations of particles containing monomeric radicals, n_1^M.

The introduction of a sharp transition from zero-one to pseudo-bulk at the cross-over radius introduces an unphysical discontinuity in the size dependence of $\bar{n}$ at r_{co}, and hence an unphysical sharp change in the particle size distribution $n(r)$ at this radius. This could be avoided by introducing a smoothing function at r_{co}. However, the presence of this sharp change does not have a significant effect on the principle variables of interest here, viz. the overall rate and the particle number density.

Coagulation rate coefficients are modeled using DLVO theory as appropriate for very small particles (see Ref. [19] for details). It is admitted that the quantitative applicability of this particular implementation of DLVO theory to such particles is questionable (e.g. [78,79]). However, it is noted that the predicted effect of inclusion of coagulation on the final particle size distribution is not large, although significant, and that the use of DLVO theory at this level is taken as acceptable for the modeling purposes of this paper (better, but more computationally complex, DLVO treatments are available, e.g. [80–82], which could be implemented if desired). While a number of parameters are required for the DLVO treatment used here [5,19,83–85], the only one whose value is uncertain and to which the results are sensitive is the Hamaker constant [86].

2.3.3. Termination rate coefficients

The simulation of pseudo-bulk particle behavior requires calculation of $\langle k_t \rangle$ in Eq (19). This uses a model discussed in detail elsewhere [28], which has been found to give acceptable accord to data such as appropriate molecular weight distributions and γ relaxation rates which are sensitive to this quantity [35]. A summary is as follows. R_i denotes the population of radicals with degree of polymerization i, and k_t^{ij} the termination rate coefficient between radicals of degree of polymerization i and j. One has:

$$\langle k_t \rangle = \frac{\sum_i \sum_j k_t^{ij} R_i R_j}{\left(\sum_i R_i \right)^2} \tag{26}$$

The value of k_t^{ij} is found using the diffusion model cited above, with Eq. (23) extended to take into account the mobility of both chains:

$$k_t^{ij} = 2p\sigma p_{spin}(D_i + D_j) \tag{27}$$

with all parameters otherwise determined as described in

Section 2.3.1. The values of R_i were found from solution of the appropriate rate equations, using the method of Clay and Gilbert [31]:

$$\frac{dR_i}{dt} = (k_p^{i-1}R_{i-1} - k_p^i R_i)C_p - k_{tr}C_p R_i - 2R_i \sum_{j=1}^{\infty} k_t^{ij} R_j \quad (28)$$

These equations, in their steady-state form ($dR_i/dt = 0$), are solved numerically by iterative solution, using a binning technique [31].

2.4. Strategy

There are two parameters whose values need to be determined by fitting appropriate experimental data: k_p^1 (the propagation rate coefficient for the monomeric radical formed from transfer), and the cross-over radius, r_{co}. For the butyl acrylate system, k_p^1 should be at most a few times the long-chain value, and r_{co} should be in the range 15–25 nm. The values of these parameters were obtained in the next section from appropriate data in a butyl acrylate seeded emulsion polymerization (i.e. emulsion polymerization in the presence of a preformed seed latex, with no new particles being formed). The values of k_p^1 and r_{co} so obtained are then used to predict rates and particle size distributions in ab initio (i.e. unseeded) systems, which are then compared to experiment. This comparison is without any adjustable parameters, and thus provides a test of the applicability of the model used.

3. Experiment

3.1. Data for parameter determination

Two types of rate data in seeded emulsion polymerization will be considered for the determination of k_p^1 and r_{co} : the steady-state rate with a chemical initiator, and the rate behavior with initiation by γ radiolysis and subsequent removal from the radiation source. The latter 'relaxation' experiments provide data which are sensitive to radical loss processes [34,87–89]. In the present system, the dominant radical-loss in a relaxation experiment will be exit followed by termination of the desorbed radical. The rate behavior for radical loss is expected to be sensitive to k_p^1 (Eq. (9)).

3.1.1. Chemically-initiated rate in seeded butyl acrylate emulsion polymerization

Data for the steady-state rate in a seeded emulsion polymerization of butyl acrylate have been given by Maeder and Gilbert (with the object of determining the transfer rate coefficient) [68]. The seed used was polystyrene, for which seed particles of very small size were available, with approximate average radius of 15 nm, but with a relatively high size polydispersity. This 'heteroseeded' emulsion polymerization assumes full compatibility between the pre-existing polystyrene and the newly formed poly(butyl acrylate); this should be an adequate approximation at low to moderate conversion [90], because butyl acrylate monomer is soluble in both polymers. The experiments were carried out at 50 °C, with $N_p = 8.3 \times 10^{17}\ l^{-1}$, and potassium persulfate as initiator at a concentration $[KPS] = 6.3 \times 10^{-4}$ M. Polymerization rate and $\bar{n}$ (where here $\bar{n}$ is the average over all particle sizes, rather than being for a single size, as in Eq. (19)) are related by:

$$R_p = -\frac{dn_M}{dt} = k_p C_p \bar{n} \frac{N_p}{N_A} \quad (29)$$

where n_M = number of moles of monomer per unit volume of aqueous phase.

To obtain estimates of the fitting parameters k_p^1 and r_{co}, Maeder and Gilbert's rate data were modeled using the description given above. The relatively high polydispersity is the reason that it is necessary to use the full particle size distribution equations, rather than the simple kinetic analysis using equations in $\bar{n}$ which can be used for seeded data with narrow size distributions. In this data fitting, it was assumed that no new particles were formed (as indeed predicted by the modeling). The parameters used are listed in Table 1. The experimental particle size distribution for this latex was measured by analytical ultracentrifugation [91,92], and is shown in Fig. 3. This particle size distribution furnishes one of the inputs in the modeling. The calculated dependence of the steady-state value of $\bar{n}$ as a function of cross-over radius is shown in Fig. 4, for two different assumed values of k_p^1. The value range for the cross-over radius giving agreement with experiment is 20–25 nm. The steady-state $\bar{n}$ calculated for $k_p^1 = 2k_p$ and $k_p^1 = k_p$ shows no strong dependence on k_p^1. This is because k_p for butyl acrylate is very high, and hence monomeric radicals propagate to much longer chains very quickly. Since termination is controlled by long–long and intermediate–long processes, $\langle k_t \rangle$ is insensitive to changes in k_p^1. It is noted that this implies that for this set of conditions (steady-state

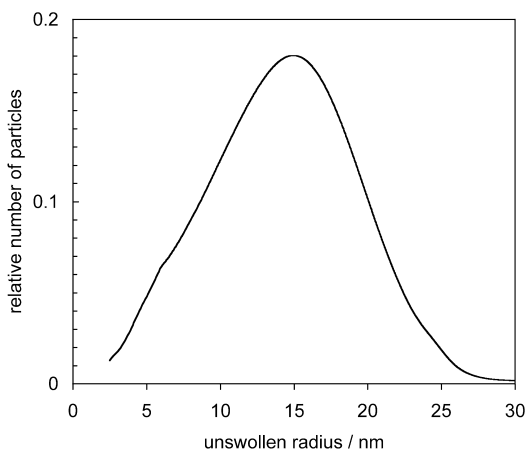

Fig. 3. Particle size distribution of the seed latex used in the experiments to obtain rate data for parameter fitting, obtained using analytic ultracentrifugation.

Table 1
Parameters used in modeling for butyl acrylate emulsion polymerization at 50 °C

Quantity	Value	Reference
k_d for $K_2S_2O_8$	1×10^{-6} s^{-1}	[96]
Radius of micelle of SDS	2.6 nm	Estimated; modeling results are insensitive to this quantity
Critical micelle concentration in the presence of monomer	3×10^{-3} M	[97]
n_{agg}	150	Assumed the same as for styrene [98]; modeling results are insensitive to this quantity
a_S (Langmuir adsorption isotherm parameter—area per surfactant molecule)	0.79 nm^2	[83]
b (Langmuir adsorption isotherm parameter)	2100 M^{-1}	[84]
Stern layer thickness	0.14 nm	[5,85]
C_p^∞	5.0 M	[77]
r_F	8 nm	[19]
C_w	6.4×10^{-3} M	[99]
j_{crit}	5	[38]
z	3	[38,100]
Cross-over radius	25 nm	This work
d_P	1.026 g cm^{-3}	[101]
d_M	0.869 g cm^{-3}	[101]
Hamaker constant	2×10^{-20} J	[86]
σ = van der Waals radius of monomer	0.7 nm	[68]
$k_{p,w}^i$	2.4×10^4 M^{-1} s^{-1}	All aqueous-phase k_p assumed equal and to have same value as in bulk [36,37]
k_p	2.4×10^4 M^{-1} s^{-1}	[36,37]
k_p^1	4.8×10^4 M^{-1} s^{-1}	This work
k_p^1, $i \geqq 2$	2.4×10^4 M^{-1} s^{-1}	Assumed that all $k_p^i = k_p$, $i \geqq 2$
k_{tr}	1.55 M^{-1} s^{-1}	[68]
D_w	1.7×10^{-5} cm^2 s^{-1}	[102]

polymerization with a relatively high radical flux), the major contribution to the kinetic behavior is pseudo-bulk. As will be seen later, for the same latex under relaxation conditions, when the radical flux becomes much lower, the major kinetic contribution is from zero-one behavior.

The data from the steady-state chemically initiated seeded system from Maeder and Gilbert thus furnish a value for r_{co}. Comparison between this value and the simulations of Fig. 2 suggests that the probability simulation gives a good first estimate for r_{co}.

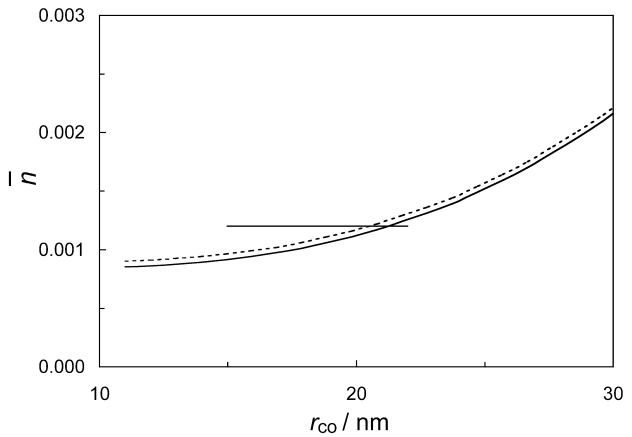

Fig. 4. Calculated $\bar{n}$ as a function of cross-over radius, for seeded butyl acrylate, using parameters given in text. Full line: k_p^1 = long-chain value of k_p (2.4×10^4 M^{-1} s^{-1}; corresponding value of $\langle k_t \rangle = 10^{7.92}$ M^{-1} s^{-1}); broken line: $k_p^1 = 2 \times$ long-chain value of k_p (corresponding value of $\langle k_t \rangle = 10^{7.93}$ M^{-1} s^{-1}). The horizontal bar is the experimentally observed value of $\bar{n}$ [68].

The experimental results for butyl acrylate in a seeded system revealed an interesting problem [68]: the value of $\bar{n}$ measured (1.2×10^{-3}) did not match the value predicted for either zero-one kinetics (0.03) or pseudo-bulk kinetics (4×10^{-4}). Maeder and Gilbert suggested that the system was controlled by kinetics somewhere between strict zero-one and pseudo-bulk. It is indeed seen here that this apparent anomaly can be explained in terms of the seeded system, which has a relatively broad particle size distribution, straddling the cross-over radius, so that the dominant kinetic mechanism is different for different sized particles.

3.1.2. Gamma relaxation experiments on a seeded butyl acrylate system

Although various attempts have been made to measure k_p^1 (e g. [93]), no definitive data are available for the present system. The value of k_p^1 will be determined from γ relaxation experiments. These were on the same seed latex as used by Maeder and Gilbert, with a particle number of 5.3×10^{17} l^{-1}. The experiment was performed at 50 °C. The surfactant was Aerosol MA at 1.8×10^{-3} M (National Starch & Chemical). Butyl acrylate (Aldrich) was prepared

for use by filtration through basic silica, distilled under reduced pressure at about 70 °C and stored at 4 °C until use (within 4 days). The internal temperature of the reaction vessel was monitored throughout the run, and the observed exotherm was insufficient to cause a significant change in reaction volume [94]. The change in $\bar{n}$ after initiation ceases was then calculated; the data so obtained are shown in Fig. 5.

The relaxation part of these data (i.e. $\bar{n}(t)$) after removal from the radiation source) will be used to find k_p^1 by fitting to the model. It was found that an efficient way of implementing this was to first fit both experimental data and simulated $\bar{n}(t)$ using the empirical expression found by comparing the zero-one and pseudo-bulk expressions for $\bar{n}(t)$ for a monodisperse latex (denoted Limit 2a and Limit 3 [34,95]), both of which have the functional form:

$$\frac{d\bar{n}}{dt} = \rho_{spont} - 2k'\bar{n}^2 \quad (30)$$

where k' is a phenomenological second-order rate coefficient for radical loss, and the entry frequency is that appropriate for spontaneous radical generation, as applicable after removal of the reactor vessel from the radical-generating ^{60}C γ source. Eq. (30) can be fitted to the time dependence of $\bar{n}$ either by least-squares fitting the analytical solution of this equation, or by using the slope-and-intercept method [34]. The experimental empirical second-order rate coefficient for radical loss so obtained (see Fig. 5) was 4.05 s^{-1}, with $\rho_{spont} = 1.8 \times 10^{-6}$ s^{-1}. This value for ρ_{spont} in the present system of butyl acrylate in a small polystyrene seed is much smaller than found for systems such as styrene-large polystyrene seed [40,41,87].

It is then possible to calculate k' for these relaxation conditions using the full model as given above (except that there is no initiator present, only ρ_{spont}), varying k_p^1 within an acceptable range. For styrene at 50 °C, relaxation data can be fitted using $k_p^1 = 4k_p$ (the long-chain value of the propagation rate coefficient) [76]. There are good reasons based on transition-state theory [74] for k_p^1 to be up to a few times this long-chain value, for any monomer. Using the full model to simulate the time evolution of $\bar{n}$ yields numerical data whence a value of k' can be extracted in the same way as for the experimental data. The calculated variation of with k_p^1 so obtained is shown in Fig. 6. A strong dependence on k_p^1 is evident in this system under relaxation conditions, in contrast to the behavior of the same system under steady-state conditions. This difference is simply ascribed to the largest component of the kinetics being zero-one under low radical flux, and pseudo-bulk for high radical flux, as discussed in the preceding section. From the results in Fig. 6, the value of k_p^1 was chosen to be twice the long-chain k_p.

3.2. Data for model testing

Ab initio emulsion polymerizations were performed in a batch reactor at 50 °C, under slight positive pressure of nitrogen. Butyl acrylate monomer was supplied by BASF, vacuum distilled at 50 °C and used within 24 h of distillation. The system contained 10% butyl acrylate, by total mass of the system. The water used was purified to Milli-Q standard. The initiator was potassium persulfate from Peroxid-Chemie GmbH (Pullach, Germany). The surfactant used was sodium dodecyl sulfate (SDS) and a commercial product sold as Texapon K 12 PA 15 (approximately 15% aqueous solution of SDS) by Henkel KgaA was used in these experiments. The surfactant concentrations were above the critical micelle concentration.

All components except the initiator were placed in the reactor vessel under a positive pressure of nitrogen and allowed to equilibrate thermally for approximately one hour. After this time, the initiator solution was added. Samples were then taken periodically by syringe, and allowed to cool to room temperature. The samples were 15 or 20 ml in volume, to which 1 ml of 0.1% hydroquinone

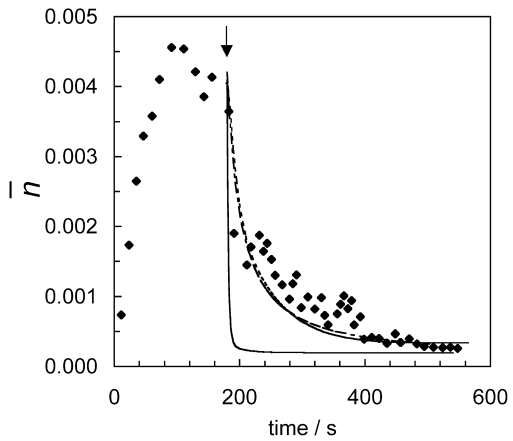

Fig. 5. Average number of radicals per particle from γ relaxation experiment. Points: experiment (arrow denotes time of removal from source). Lines: calculated from full model, with $k_p^1 = k_p$ (—) and $2k_p$ (…), and (–·–·) by fitting to Eq. (30) with $k' = 4.05$ s^{-1} and $\rho_{spont} = 1.8 \times 10^{-6}$ s^{-1}.

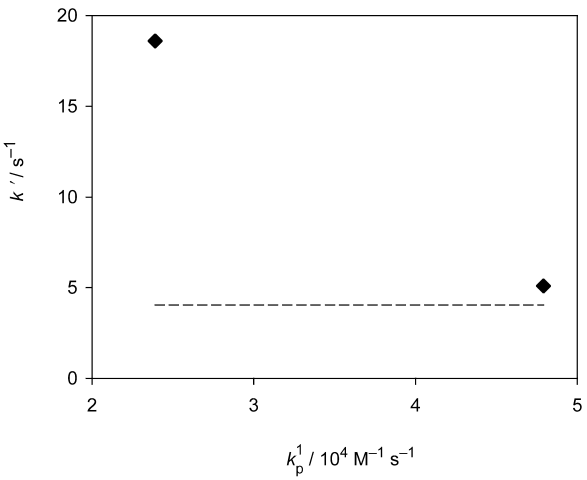

Fig. 6. Points: calculated dependence of the empirical radical loss rate coefficient k' (Eq. (30)) on input value of k_p^1 in simulation of γ radiolysis relaxation. Horizontal line: value obtained by fitting Eq. (30) to experiment.

solution was added. Polymerization was assumed to cease with exposure to oxygen and hydroquinone and cooling to room temperature. Gravimetry was performed on the samples to monitor conversion, with samples being dried at 50 °C for 12 h, to remove all traces of water and residual monomer. The final solids content was 10%.

In order to obtain particle sizes and hence number of particles, two methods were utilized: capillary hydrodynamic fractionation (CHDF) and analytical ultracentrifuge (AUC). CHDF measurements were usually made within 2 days of polymerization, using a CHDF-110 Particle Size Analyzer from Matec (Hopkinton, MA). The samples were prepared by diluting the latex to 0.5% solids with eluent (0.1% Brij 35 solution, 0.005% SDS with a conductivity of 9 $\mu S\ cm^{-1}$). The AUC apparatus was a XL-E from Beckman Instruments (Palo Alto, CA) with interference optics detector.

4. Comparison of model predictions with experiment

4.1. Parameters for modeling

The parameters used in modeling butyl acrylate are listed in Table 1. As noted also for styrene [35], the average termination rate coefficient $\langle k_t \rangle$, which is calculated within the model, is not strongly dependent on initiator concentration: e g., the calculated values for 10^{-3} and 10^{-2} M initiator are $\langle k_t \rangle = 10^{7.90}$ and $10^{7.92}\ M^{-1}\ s^{-1}$, respectively, at $w_p = 0.4$. For this butyl acrylate system, which is always rubbery, the calculated dependence on w_p is also very weak.

4.2. Quantitative comparison

Fig. 7 compares observed and predicted final particle number as a function of initiator concentration. It is seen that the accord is quite acceptable.

Fig. 8 shows particle number and size as functions of time. Modeled and observed time for nucleation and the time evolution of particle diameter are in reasonable, but not perfect agreement, with fast initial nucleation and a subsequent period of slow particle formation. It is noted that CHDF is only semi-quantitative for the smallest particle size in this data set, and the uncertainty in size measurement for this sample leads to such a large error in the value of N_p (which from Eq. (3) is three times the uncertainty in radius) that the nominal value N_p for this smallest size, not shown in Fig. 8, is greater than the long-time value; the uncertainty in this nominal value is, however, so large that it is quite unreliable.

Fig. 9 shows that there is good agreement between predicted and experimental conversion as a function of time.

Comparison of the observed and simulated particle number as a function of surfactant concentration shown in Fig. 10 shows a good agreement, the predicted value being well within a factor of two of observation.

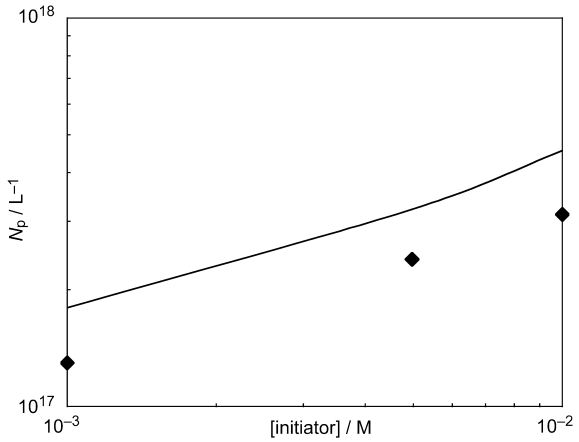

Fig. 7. Observed (points) and predicted (line) final particle number as a function of initiator (potassium persulfate) concentration for butyl acrylate at 50 °C, SDS concentration = 1×10^{-2} M.

5. Conclusions

A model has been given for the a priori prediction of particle number and rate, and hence particle size, in an emulsion polymerization system in which pseudo-bulk as well as zero-one kinetics need to be taken into account during the period of particle formation. This is necessary for monomers such as acrylates, which have such a high propagation rate coefficient that it is possible to have two or more growing radicals co-existing for a significant time in quite small particles. The reason for this is the chain-length dependence of the termination rate coefficient, where a long chain diffuses slowly and thus terminates slowly, and so the rate of termination is slowed down if a chain is able to undergo extensive propagation before it is eventually

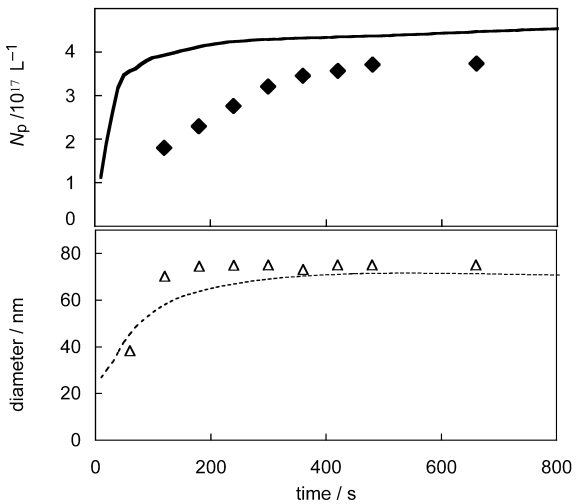

Fig. 8. Particle number and diameter as functions of time, for 10% solids butyl acrylate, with SDS concentration = 1×10^{-2} M and initiator (KPS) concentration 1×10^{-2} M. A one-minute inhibition period was subtracted from the experimental data. Points: experiment; lines: simulated.

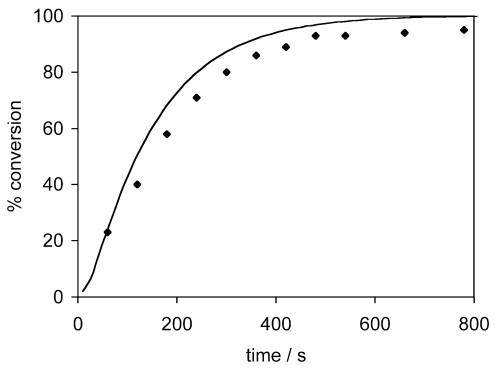

Fig. 9. Percentage conversion as a function of time, for the system of Fig. 8. A one-minute inhibition period was subtracted from the experimental data. Points: observed; line: simulated.

terminated. The present model is an extension of a previous treatment which takes all the complex events in emulsion polymerization into account in zero-one systems (where one cannot have significant co-existence of two radicals in the same particle). The novel step in the present treatment is to include pseudo-bulk kinetics in the time evolution of the particle size distribution. The chain-length dependence of termination is taken into account through an average termination rate coefficient, where the average is over the distribution of growing radicals of different degrees of polymerization.

The model perforce contains a number of parameters whose values are uncertain. Those to which the primary variables of interest (the overall rate and the particle number) are sensitive are the cross-over radius r_{co}, and the rate coefficient for propagation of a monomeric radical, k_p^1. While these can in principle be found independently from appropriate data, in practice such data are not yet available for systems of interest. The present treatment therefore evaluates these from measurements on *seeded* systems, for subsequent use in prediction of properties of ab initio emulsion polymerizations. If such seeded data are not available, reasonable estimates of each quantity can be

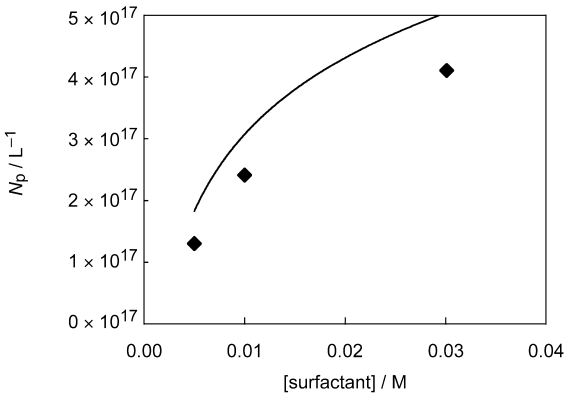

Fig. 10. The final particle number for 10% solids butyl acrylate as a function of the concentration of SDS surfactant. The initiator used was potassium persulfate, at a concentration of 5×10^{-3} M. Points: observed; line: simulated.

made. Thus, k_p^1 is likely to be 2–4 times the long-chain k_p, and an approximate estimate of r_{co} from cumulative probability plots such as those given in Fig. 2.

It is found that for the case of butyl acrylate emulsion polymerization, experiment and model are in good, but not perfect, agreement for rate and for particle number (and hence particle size). This accord is consistent with the quantitative applicability of the physical models used in the formulation.

Acknowledgements

The support of BASF AG, and excellent interaction and discussions with Drs Dieter Distler, Jürgen Schmidt-Thuemmes and Bart Manders of that company, are gratefully acknowledged. The Key Centre for Polymer Colloids is established and supported under the Australian Research Council's Research Centres program. For the γ radiolysis experiments, support from the Australian Nuclear Science and Technology Organization is gratefully acknowledged, as is help from David Sangster. Stuart Prescott's help in correcting the probability calculations is also much appreciated.

References

[1] Priest WJ. J Phys Chem 1952;56:1077.
[2] Fitch RM, Tsai CH. In: Fitch RM, editor. Polymer colloids. New York: Plenum; 1971. p. 73.
[3] Ugelstad J, Hansen FK. Rubber Chem Technol 1976;49:536.
[4] Smith WV, Ewart RH. J Chem Phys 1948;16:592.
[5] Feeney PJ, Napper DH, Gilbert RG. Macromolecules 1987;20:2922.
[6] Richards JR, Congalidis JP, Gilbert RG. J Appl Polym Sci 1989;37:2727.
[7] Coen EM, Gilbert RG. In: Asua JM, editor. Polymeric dispersions. Principles and applications. Dordrecht: Kluwer Academic; 1997. p. 67.
[8] Casey BS, Morrison BR, Gilbert RG. Prog Polym Sci 1993;18:1041.
[9] Giannetti E. Macromolecules 1990;23:4748.
[10] Schlüter H. Colloid Polym Sci 1993;271:246.
[11] Schlüter H. Macromolecules 1990;23:1618.
[12] Hansen FK, Ugelstad J. J Polym Sci, Polym Chem Ed 1978;16:1953.
[13] Fitch RM, Palmgren TH, Aoyagi T, Zuikov A. Angew Makromol Chemie 1984;123/124:261.
[14] Hansen FK. Chem Engng Sci 1993;48:437.
[15] Dougherty EP. J Appl Polym Sci 1986;32:3051.
[16] Dougherty EP. J Appl Polym Sci 1986;32:3079.
[17] Hansen FK, Ugelstad J. J Polym Sci, Polym Chem Ed 1979;17:3033.
[18] Tauer K, Kühn I. Macromolecules 1995;28:2236.
[19] Coen EM, Gilbert RG, Morrison BR, Peach S, Leube H. Polymer 1998;39:7099.
[20] Fontenot K, Schork FJ. Polym React Engng 1992;1:75.
[21] Herrera-Ordonez J, Olayo R. J Polym Sci, Part A—Polym Chem 2000;38:2201.
[22] Herrera-Ordonez J, Olayo R. J Polym Sci, Part A—Polym Chem 2001;39:2547.
[23] Gao J, Penlidis A. Prog Polym Sci 2002;27:403.
[24] Tauer K. Surf Sci Ser 2001;100:429.
[25] Fitch RM, Shih LB. Prog Colloid Polym Sci 1975;56:1.

[26] Hansen FK, Ugelstad J. In: Piirma I, editor. Emulsion polymerization. New York: Academic; 1982.
[27] Richards JR, Congalidis JP, Gilbert RG. In: Provder T, editor. ACS Symposium Series (computer applications in applied polymer science), Washington, DC: American Chemical Society; 1989. p. 360.
[28] Russell GT, Gilbert RG, Napper DH. Macromolecules 1992;25: 2459.
[29] Brandrup J, Immergut EH, Grulke EA, editors. Polymer handbook. New York: Wiley; 1999.
[30] Prescott SW. Macromolecules 2003;36:9608.
[31] Clay PA, Gilbert RG. Macromolecules 1995;28:552.
[32] Tobita H. Macromolecules 1995;28:5128.
[33] Casey BS, Morrison BR, Maxwell IA, Gilbert RG, Napper DH. J Polym Sci, Part A: Polym Chem 1994;32:605.
[34] Gilbert RG. Emulsion polymerization: a mechanistic approach. London: Academic; 1995.
[35] Clay PA, Christie DI, Gilbert RG. In: Matyjaszewski K, editor. Advances in free-radical polymerization. Washington, DC: American Chemical Society; 1998. p. 104.
[36] Lyons RA, Hutovic J, Piton MC, Christie DI, Clay PA, Manders BG, Kable SH, Gilbert RG. Macromolecules 1996;29:1918.
[37] Beuermann S, Paquet DA, McMinn JH, Hutchinson RA. Macromolecules 1996;29:4206.
[38] Maxwell IA, Morrison BR, Napper DH, Gilbert RG. Macromolecules 1991;24:1629.
[39] DRAFT IUPAC terminology on polymer colloids: http://www.kcpc.usyd.edu.au/resources/IUPAC_polym_coll_terminology.pdf.
[40] Hawkett BS, Napper DH, Gilbert RG. J Chem Soc, Faraday Trans 1 1980;76:1323.
[41] Christie DI, Gilbert RG, Congalidis JP, Richards JR, McMinn JH. Macromolecules 2001;34:5158.
[42] Prescott SW, Ballard MJ, Rizzardo E, Gilbert RG. Macromolecules 2002;35:5417.
[43] Ferguson CJ, Hughes RJ, Pham BTT, Hawkett BS, Gilbert RG, Serelis AK, Such CH. Macromolecules 2002;35:9243.
[44] Ugelstad J, Mørk PC, Dahl P, Rangenes P. J Polym Sci, Part C 1969; 27:49.
[45] Nomura M, Harada M, Nakagawara K, Eguchi W, Nagata S. J Chem Engng Jpn 1970;4:160.
[46] Nomura M, Harada M, Eguchi W, Nagata S. J Appl Polym Sci 1971; 15:675.
[47] Plessis C, Arzamendi G, Leiza JR, Schoonbrood HAS, Charmot D, Asua JM. Macromolecules 2000;33:4.
[48] Britton DJ, Lovell PA, Heatley F, Venkatesh R. Macromol Symp 2001;175:95.
[49] Couvreur L, Piteau G, Castignolles P, Tonge M, Coutin B, Charleux B, Vairon JP. Macromol Symp 2001;174:197.
[50] Plessis C, Arzamendi G, Alberdi JM, van Herk AM, Leiza JR, Asua JM. Macromol Rapid Commun 2003;24:173.
[51] Barouch E, Matijevic E, Wright TH. J Chem Soc, Faraday Trans I 1985;81:1819.
[52] Barouch E, Matijevic E. J Chem Soc, Faraday Trans I 1985;81:1797.
[53] Lichti G, Gilbert RG, Napper DH. J Polym Sci, Polym Chem Ed 1983;21:269.
[54] Lichti G, Hawkett BH, Gilbert RG, Napper DH, Sangster DF. J Polym Sci, Polym Chem Ed 1981;19:925.
[55] Morton M, Kaizerman S, Altier MW. J Colloid Sci 1954;9:300.
[56] Maruthamuthu P. Makromol Chem, Rapid Commun 1980;1:23.
[57] McAskill NA, Sangster DF. Aust J Chem 1979;32:2611.
[58] McAskill NA, Sangster DF. Aust J Chem 1984;37:2137.
[59] Koltzenburg G, Bastian E, Steenken S. Angew Chem, Int Ed Engl 1988;27:1066.
[60] Neta P, Huie RE, Ross A. J Phys Chem Ref Data 1988;17:1027.
[61] Clifton CL, Huie RE. Int J Chem Kinet 1989;21:677.
[62] Morrison BR, Maxwell IA, Gilbert RG, Napper DH. In: Daniels ES, Sudol ED, El-Aasser M, editors. ACS Symposium Series—polymer latexes—preparation, characterization and applications. Washington, DC: American Chemical Society; 1992. p. 28.
[63] Morrison BR, Gilbert RG. Macromol Symp 1995;92:13.
[64] Coen E, Lyons RA, Gilbert RG. Macromolecules 1996;29:5128.
[65] Russell GT, Gilbert RG, Napper DH. Macromolecules 1993;26: 3538.
[66] Benson SW, North AM. J Am Chem Soc 1962;84:935.
[67] Russell GT. Aust J Chem 2002;55:399.
[68] Maeder S, Gilbert RG. Macromolecules 1998;31:4410.
[69] Gilbert RG, Smith SC. Theory of unimolecular and recombination reactions. Oxford and Cambridge Mass: Blackwell Scientific; 1990.
[70] Griffiths MC, Strauch J, Monteiro MJ, Gilbert RG. Macromolecules 1998;31:7835.
[71] Piton MC, Gilbert RG, Chapman BE, Kuchel PW. Macromolecules 1993;26:4472.
[72] Strauch J, McdDonald J, Chapman BE, Kuchel PW, Hawkett BS, Roberts GE, Tonge MP, Gilbert RG. J Polym Sci, Part A: Polym Chem Ed 2003;41:2491.
[73] Hutchinson RA, Paquet DA, McMinn JH, Fuller RE. Macromolecules 1995;28:4023.
[74] Heuts JPA, Radom L, Gilbert RG. Macromolecules 1995;28:8771.
[75] Heuts JPA, Gilbert RG, Radom L. J Phys Chem 1996;100:18997.
[76] Morrison BR, Casey BS, Lacík I, Leslie GL, Sangster DF, Gilbert RG, Napper DH. J Polym Sci, Part A: Polym Chem 1994;32:631.
[77] Gordon R. Honors Thesis. Sydney University; 1990.
[78] Ottewill RH, Shaw JN. Discuss Faraday Soc; 1966, No. 42:154.
[79] Kostansek EC. Trends Polym Sci 1996;4:383.
[80] Behrens SH, Christl DI, Emmerzael R, Schurtenberger P, Borkovec M. Langmuir 2000;16:2566.
[81] Scales PJ, Johnson SB, Healy TW, Kapur PC. AIChE J 1998;44:538.
[82] Peula JM, Fernandez-Barbero A, Hidalgo-Alvarez R, de las Nieves FJ. Langmuir 1997;13:3938.
[83] Sütterlin N. In: Fitch RM, editor. Polymer colloids II. New York: Plenum; 1980. p. 583.
[84] Ahmed SM, El-Aasser MS, Micale FJ, Poehlein GW, Vanderhoff JW. In: Fitch RM, editor. Polymer colloids II. New York: Plenum; 1980. p. 265.
[85] Dunn AS, Chong LCH. Br Polym J 1970;2:49.
[86] Hough DB, White LR. Adv Colloid Interface Sci 1980;14:3.
[87] Lansdowne SW, Gilbert RG, Napper DH, Sangster DF. J Chem Soc, Faraday Trans 1 1980;76:1344.
[88] Ballard MJ, Napper DH, Gilbert RG, Sangster DF. J Polym Sci, Polym Chem Ed 1986;24:1027.
[89] Adams ME, Russell GT, Casey BS, Gilbert RG, Napper DH, Sangster DF. Macromolecules 1990;23:4624.
[90] Schoonbrood HAS, German AL, Gilbert RG. Macromolecules 1995; 28:34.
[91] Colfen H, Pauck T. Colloid Polym Sci 1997;275:175.
[92] Harding SE. Trends Anal Chem 1994;13:439.
[93] Beckwith ALJ, Poole JS. J Am Chem Soc 2002;124:9489.
[94] De Bruyn H, Gilbert RG, Ballard MJ. Macromolecules 1996;29: 8666.
[95] Casey BS, Mills MF, Sangster DF, Gilbert RG, Napper DH. Macromolecules 1992;25:7063.
[96] Kolthoff IM, Miller IK. J Am Chem Soc 1951;73:3055.
[97] Janssen RQF, van Herk AM, German AL. JOCCA-Surf Coat Int 1993;76:455.
[98] Giannetti E. AIChE J 1993;39:1210.
[99] Capek I, Barton J, Ordinova E. Chem Zvesti 1984;38:802.
[100] Gilbert RG. In: Lovell PA, El-Aasser MS, editors. Emulsion polymerization and emulsion polymers. London: Wiley; 1997. p. 165.
[101] Maxwell IA, Napper DH, Gilbert RG. J Chem Soc, Faraday Trans 1 1987;83:1449.
[102] Wilke CR, Chang P. AIChE J 1955;1:264.